3D Analysis of Steep Slopes Subjected to Seismic Excitation

S.S. Nadukuru[1], T. Martel[1], Student Members ASCE, and R.L. Michalowski[2], F.ASCE

[1]University of Michigan, Department of Civil and Environmental Engineering, Ann Arbor, MI 48109-2125, U.S.A.; siddu@umich.edu
[2]University of Michigan, Department of Civil and Environmental Engineering, Ann Arbor, MI 48109-2125, U.S.A.; rlmich@umich.edu, tel: 734 763-2146, fax: 734 764-4292

ABSTRACT

Design of slopes and analysis of existing slopes are carried out routinely using approximations of plane strain and substitution of quasi-static load for the seismic excitation. A three-dimensional analysis of slopes is used here, based on the kinematic theorem of limit analysis. A 3D rotational mechanism with a failure surface passing through the slope toe was developed, applicable to steep slopes. A quasi-static approach is used and an example of charts for the assessment of the factor of safety for slopes with predefined width of the failure mechanism is shown. Critical acceleration is also calculated for 3D slopes, and a sliding block analysis is carried out to develop a solution for displacements of slopes subjected to seismic excitation.

INTRODUCTION

The methods developed for 3D analyses of slope stability can be grouped in at least three categories: limit equilibrium approach, numerical methods, and limit analysis. In the first category the failing mass is divided into blocks (typically columns), and global (force) equilibrium is required (*e.g.*, Hungr 1987). As the problem is statically indeterminate, additional static, often arbitrary assumptions are made. The second category includes predominantly the finite element method (*e.g.*, Griffiths and Marquez 2007). The advantage of FEM is in assessment of deformation prior to failure, and no need to predetermine the failure pattern. This method is well-suited to produce solutions for specific, well-defined slopes, but it becomes more elaborate when multiple calculations are needed with varied slope geometry. Finally, the limit analysis approach can yield a rigorous bound to the safety factor. While approximate, optimization of the failure mechanism assures that the solution is a good estimate of the 'true' safety factor. This was confirmed by calculations of Chen (1975), who concluded that the rotational mechanism for slopes failing under plane strain conditions is the most critical one. Similar conclusions follow from comparisons of limit analysis results and the finite element calculations (*e.g.*, Lane and Griffiths 1997). The kinematic approach of limit analysis is used in this presentation.

We limit application of the results to steep slopes as the failure mechanism considered always passes though the toe; this may not be true of 'gentle' slopes. Efforts to produce a kinematically admissible 3D below-toe mechanism are underway.

After a brief introduction of the method, we present the 3D failure mechanism, followed by calculations of the safety factor for slopes subjected to seismic excitation. Limited results of critical acceleration calculations, and preliminary results from 3D sliding block analysis are also presented.

KINEMATIC APPROACH OF LIMIT ANALYSIS

Limit analysis is applicable to soils with convex yield conditions and deformation governed by the normality rule. Early applications of limit analysis to slope stability problems (2D) can be found in Drucker et al. (1952) and Drucker and Prager (1952). A multitude of solutions to a wide range of problems utilizing this method can be found in the monograph by Chen (1975).

So far, there have been only a few attempts at 3D analyses of slopes using the kinematic approach of limit analysis. These include a single and multi-block translation mechanisms (Drescher 1983, Michalowski 1989), and rotational mechanisms (de Buhan and Garnier 1998, Michalowski and Drescher 2009, Michalowski 2010). Three-dimensional failures for purely cohesive soils were considered earlier by Baligh and Azzouz (1975) and Gens et al. (1988).

A rotational mechanism of collapse is considered here as developed by Michalowski and Drescher (2009). The geometry of the failure surface is presented in Fig. 1(a), and its cross-section with the slope is illustrated in Fig. 1(b).

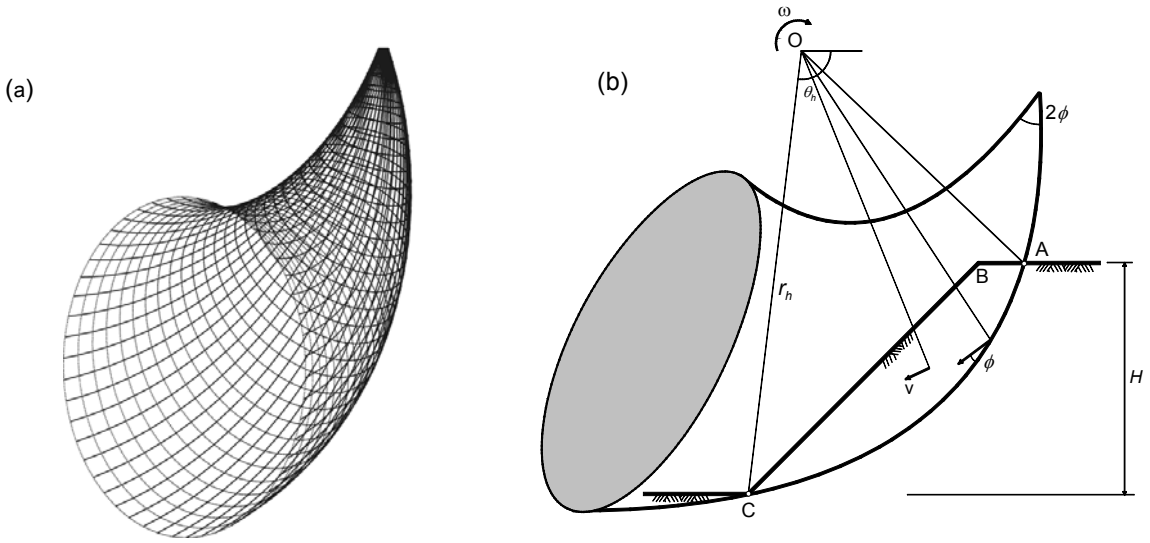

Figure 1. (a) The shape of the failure surface, and (b) schematic of the collapse mechanism.

The failure surface has a shape of a curvilinear cone ("horn") with an apex angle of 2ϕ, which assures admissibility of rigid rotation. The contours of the surface on the central cross-section are both log-spirals, and the trace of the surface on any radial plane forms a circle. The details of the analysis have already been presented elsewhere (Michalowski and Drescher 2009), and we concentrate on the inclusion of the inertial terms in the analysis. To assure that the mechanism will tend to a plane one if no limitations are placed on its width, this mechanism is modified by inserting a plane section of width *b*, Fig. 2. The geometry of the insert is such so that the entire composite surface is smooth.

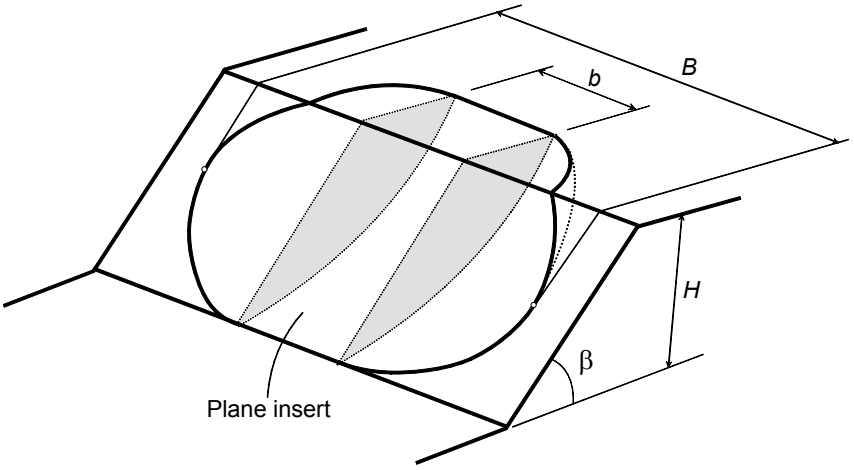

Figure 2. Collapse mechanism modified with a plane insert (adapted from Michalowski and Drescher 2009).

The kinematic approach of limit analysis is based on a theorem that states: the rate of internal work in any kinematically admissible mechanism is not smaller than the work rate of true external forces. Consequently, by equating the two rates, one can calculate a rigorous bound to one unknown, be it limit load, safety factor, or critical acceleration. In general, this inequality can be written in the following form

$$D^{3D} + D^{2D} \geq W_{\gamma}^{3D} + W_{\gamma}^{2D} + W_{s}^{3D} + W_{s}^{2D} \tag{1}$$

where superscript *3D* denotes the work rates for the three-dimensional portion of the failure mechanism and superscript *2D* relates to the plane insert (Fig. 2). The two terms on the left-hand side represent the internal work rate, whereas the subscript γ in the terms on the right-hand side denotes the rate of gravity forces, and subscript *s* relates to the seismic (inertial) force. The seismic force is taken here as the quasi-steady horizontal load of intensity equal to fraction k_h of the distributed gravity load.

SAFETY FACTOR AND CRITICAL ACCELERATION

Results of calculations based on the energy rate balance for an incipient 3D mechanism can yield the safety factor or the yield acceleration. In any case, a strict bound to only one unknown can be calculated from inequality (1). The safety factor is defined here as the ratio of the strength parameters to those needed to maintain stability (c_d, $\tan\phi_d$)

$$F = \frac{c}{c_d} = \frac{\tan\phi}{\tan\phi_d} \tag{2}$$

When the strength of the soil is described by two parameters: ϕ and c (Mohr-Coulomb yield condition), then iteration is typically required to determine the safety factor from pre-calculated charts. However, if the results are presented as function of $c/\tan\phi$, there will be no need for iteration. This is because this ratio is independent of the safety factor, *i.e.*, $c/\tan\phi = c_d/\tan\phi_d$. The preliminary results in Fig. 3 are presented as $F/\tan\phi$ (or $1/\tan\phi_d$) vs. $c/(\gamma H\tan\phi)$.

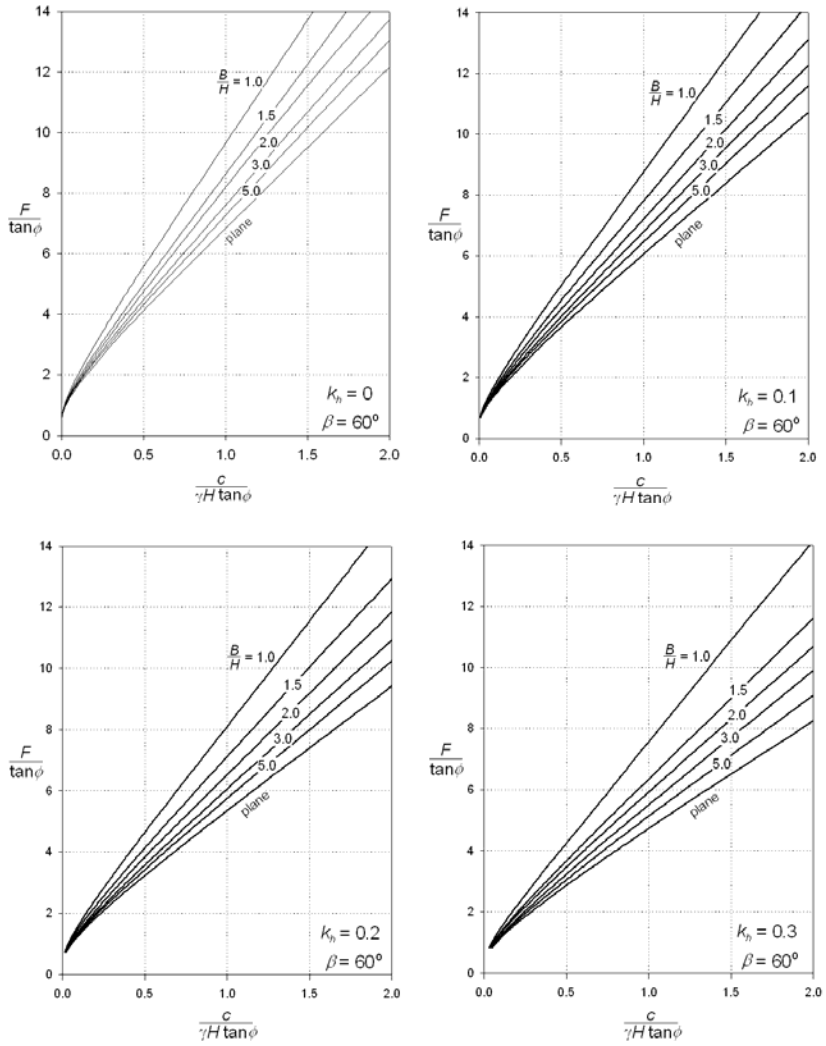

Figure 3. Safety factor for slopes with inclination angle of 60°.

Reading the safety factor from charts in Fig. 3 is straight forward: for parameter $c/(\gamma H\tan\phi)$, characteristic of a given slope, read $F/\tan\phi$ for the failure of given width B. Width B is determined by geology or geometry (*e.g.*, in case of excavation slopes). Results for a wider range of parameters will be presented elsewhere (Michalowski and Martel 2010). The advantage of these charts is in assessment of the influence of limited width of the mechanism (in case of embankment slopes, or constraints set by geology) over the 2D solutions (indicated on charts as 'plane' case).

Alternatively, the problem can be formulated in terms of critical acceleration coefficients k_y. In this case the slope is characterized by inclination angle β, internal friction angle ϕ, and coefficient $c/\gamma H$. An example of calculated critical acceleration coefficient for 60-degree slopes is illustrated in Fig. 4.

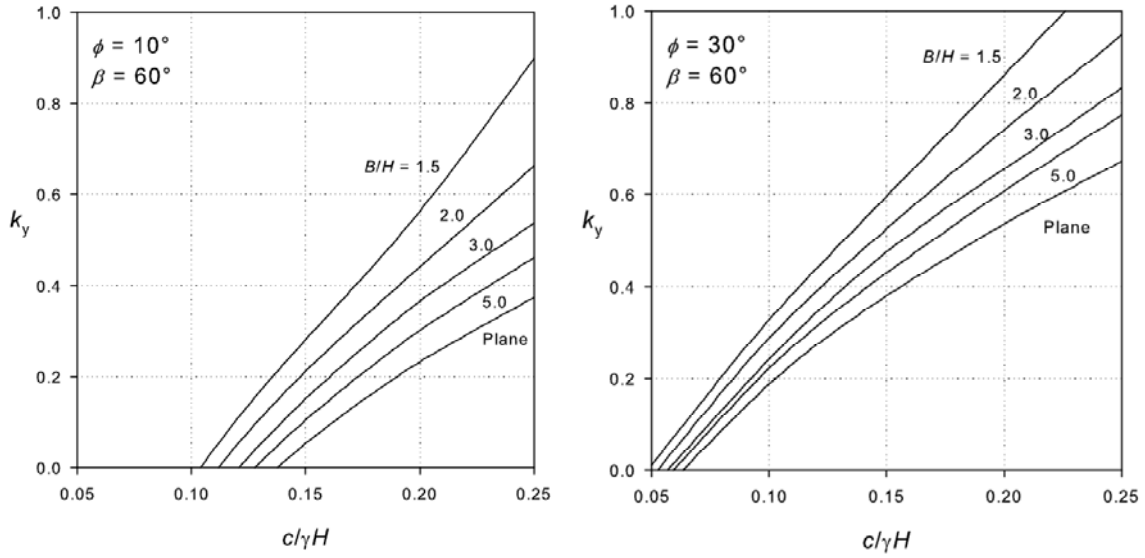

Figure 4. Critical acceleration for slopes with inclination angle of 60°.

Once the critical acceleration is determined, one can estimate displacements of slopes subjected to ground motion with acceleration exceeding the critical value. This is shown in the next section.

SLIDING BLOCK ANALYSIS

Calculations of displacements of slopes subjected to seismic acceleration are based here on the concept of a sliding block (Newmark 1965). Here, the consideration is modified to include rotation of the failing mass, much like that in the paper of Chang et al. (1984), You and Michalowski (1999), and Michalowski and You (2000). While the specific mechanism considered here is one rotating block, the concept can be applied to multi-block mechanisms as demonstrated in Michalowski (2007).

The details of the analysis will be presented elsewhere; here we present only some preliminary results. Based on the geometrical relations in Fig. 1(a), the horizontal component of the displacement at the toe can be written as

$$u_x = r_h \theta \sin \theta_h \tag{3}$$

Where both r_h and θ_h are shown in Fig. 1(a), and θ is the total angular displacement calculated from the analysis as

$$\theta = \int_t \int_t \ddot{\theta} dt dt \,, \quad \dot{\theta} > 0 \tag{4}$$

with $\ddot{\theta}$ being the angular acceleration calculated from the dynamic analysis of rigid rotation that assures that the failing slope satisfies equations of motion. Integration in eq. (4) is taken only over time intervals when the angular velocity $\dot{\theta}$ is positive. The specific form of $\ddot{\theta}$ in eq. (4) is calculated by subtracting the work rate balance equation for an incipient rotation of the slope at the moment when the record has reached the yield acceleration ($k_h = k_y$), from the balance equation for an instant when the acceleration exceeds the yield value ($k_h > k_y$). The solution to $\ddot{\theta}$ can be written in general form as

$$\ddot{\theta} = g(k - k_y) M \tag{5}$$

where M is a dimensionless coefficient dependent only on the slope characteristics, and $k - k_y$ is the difference between the acceleration coefficient in the ground motion record and the critical acceleration coefficient of the structure (here: $k = k_h$). Now, using eqs. (3) - (5), the horizontal displacement at the toe takes form

$$u_x = Cg \int_t \int_t (k - k_y) dt dt \,, \quad \dot{\theta} > 0 \tag{6}$$

where dimensionless coefficient C is a function of the slope geometry and the failure mechanism (depends on M). A more detailed derivation of a similar type, but for a 2D translational mechanism, can be found in Michalowski (2007).

Only horizontal seismic acceleration was considered in the analysis, although including the vertical component of acceleration is straight-forward. The shaking was assumed to take place in the plane of Fig. 1(a) (*i.e.*, perpendicular to the crest), with the most adverse effect when the acceleration points into the slope (inertial force out-of-slope).

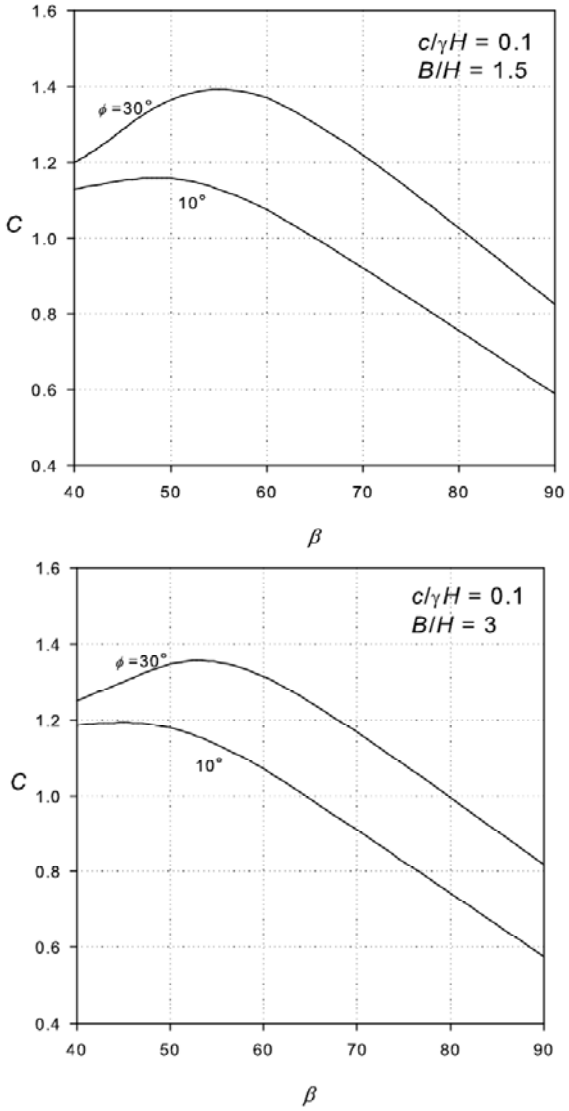

Figure 5. An example of calculated coefficient *C* for slopes characterized by $c/\gamma H = 0.1$.

The simplicity of the expression in eq. (6) comes from the dynamic analysis of the rigid-body rotation. For a given slope with a given collapse mechanism, coefficient *C* is the outcome of the analysis (Fig. 5), while the double-time integral can be pre-calculated for variety of (GPA-scaled) ground motions and critical accelerations. An example of pre-calculated integrals $g\int_t\int_t (k-k_y)dtdt$ (in cm) is shown in Fig. 6.

The Peak Ground Acceleration of the record (Imperial Valley Earthquake[1]) was scaled, and the integrals are presented in Fig. 6 for a variety of differences k_m –

[1] Station name: Holtville Post Office; mag. 6.5, Ep. dist.. 19.81 km., PGA 0.25g, PGV 47.49 cm/s, PGD 29.15 cm.

k_y. This is distinct from the more common presentation as a function of k_y/k_m, which tends to give a more non-linear representation of the displacement. In either case, the charts represent the same outcome, and any permanent displacement can occur only if $k_m \geq k_y$.

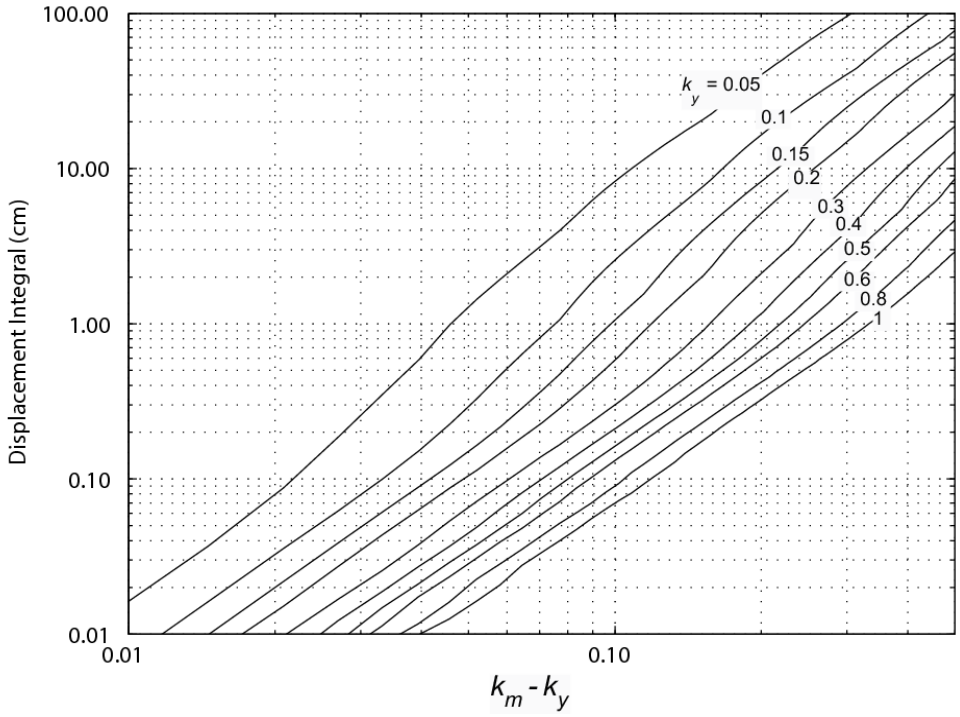

Figure 6. Pre-calculated displacement integral for 1979 Imperial Valley Earthquake[1].

The results presented are preliminary; proper analysis of seismic displacements of slopes requires calculations for many ground motions, and it might include an analysis of sensitivity of the outcome to the characteristic features of the ground motion records, such as peak ground velocity or peak ground acceleration.

CONCLUSIONS

Three-dimensional stability analysis of slopes was developed with seismic loads considered as quasi-static distributed force. The charts developed allow one to read the safety factor without a need for an iterative procedure. The analysis is applicable in cases where the width of the mechanism is limited, for instance, in case of excavations, or when the mechanism is confined by local geology. An analysis was also developed for calculations of critical acceleration coefficient and displacements due to seismic excitation. The latter calculations are based on the dynamic analysis of the rigid rotation mechanism.

A key limitation of the analysis developed is in the failure surface passing through the toe of the slope, making it applicable to slopes of inclination not smaller than 45°. Future research will address 3D below-toe failure patterns, as well as the influence of the presence of a phreatic surface in the slope.

ACKNOWLEDGEMENTS

The work presented in this paper was carried out while all authors were supported by the National Science Foundation, grant No. CMMI-0724022, and the last author was supported by the Army Research Office, grant No. W911NF-08-1-0376. This support is greatly appreciated.

REFERENCES

Baligh, M.M. & Azzouz, A.S. (1975). End effects on stability of cohesive slopes. *ASCE J. Geot. Eng. Div.*, **101**, No. GT11, 1105-1117.

Chang, C-J., Chen, W.F. and Yao, J.P. (1984). Seismic displacements in slopes by limit analysis. *J. Geot. Engrg*. **110**(7): 860-874.

Chen, W.F. (1975). Soil Plasticity and Limit Analysis. Elsevier, Rotterdam.

de Buhan, P. & Garnier, D. (1998). Three dimensional bearing capacity analysis of a foundation near a slope. *Soils and Foundations*, **38**, No. 3, 153-163.

Drescher, A. (1983). Limit plasticity approach to piping in bins. *J. Appl. Mech.*, **50**, 549-553.

Drucker, D.C. and Prager, W. (1952). Soil mechanics and plastic analysis or limit design. *Quart. Appl. Math.*, **10**(2), 157-165.

Drucker, D.C., Prager, W. & Greenberg, H.J. (1952). Extended limit design theorems for continuous media. *Quarterly of Applied Math*. **9**, 381-389.

Gens, A., Hutchinson, J.N. & Cavounidis, S. (1988). Three-dimensional analysis of slides in cohesive soils. *Géotechnique*, **38**(1), 1-23.

Griffiths, D.V. & Marquez, R.M. (2007). Three-dimensional slope stability analysis by elasto-plastic finite elements. *Géotechnique*, **57**, No. 6, 537-546.

Hungr, O. (1987). An extension of Bishop's simplified method of slope stability analysis to three dimensions. *Géotechnique*, **37**(1), 113-117.

Lane, P.A. and Griffiths, D.V. (1997). Finite element slope stability analysis – Why are engineers still drawing circles? *Proc. 6th Int. Symposium on numerical models in geomechanics* (NUMOG VI). Eds. S. Pietruszczak and G.N. Pande. Belkema, Rotterdam, 589-0593.

Michalowski, R.L. (1989). Three-dimensional analysis of locally loaded slopes. *Géotechnique*, **39**, No. 1, 27-38.

Michalowski, R.L. (2007). Displacements of multi-block geotechnical structures subjected to seismic excitation. *Journal of Geotechnical and Geoenvironmental Engineering*, **133**, No. 11, 1432-1439.

Michalowski, R.L. (2010). Limit analysis and stability charts for 3D slope failures. *Journal of Geotechnical and Geoenvironmental Engineering*, **136**, No. 4, 583-593.

Michalowski, R.L. and Drescher, A. (2009) Three-dimensional stability of slopes and excavations. *Géotechnique*, **59**, No. 10, 839-850.

Michalowski, R.L. and Martel, T. (2010). Stability charts for 3D failures of steep slopes subjected to seismic excitation. *J. Geotech. Geoenv. Engrg.*, in print.

Michalowski, R.L. and You, L. (2000). Displacement of reinforced slopes subjected to seismic loads. *Journal of Geotechnical and Geoenvironmental Engineering*, **126**, No. 8, 685-694.

Newmark, N.M. (1965). Effects of earthquakes on dams and embankments. *Géotechnique*, London, **15**, 139-160.

You, L. and Michalowski, R.L. (1999). Displacement charts for slopes subjected to seismic loads. *Computers and Geotechnics*, **25,** No. 1, 45-55.